

Achieving Wellbore Stability using Black Powders: Understanding the Mechanism

Sharath Savari, Halliburton and Arunesh Kumar (formerly Halliburton)

Copyright 2012, AADE

This paper was prepared for presentation at the 2012 AADE Fluids Technical Conference and Exhibition held at the Hilton Houston North Hotel, Houston, Texas, April 10-11, 2012. This conference was sponsored by the American Association of Drilling Engineers. The information presented in this paper does not reflect any position, claim or endorsement made or implied by the American Association of Drilling Engineers, their officers or members. Questions concerning the content of this paper should be directed to the individual(s) listed as author(s) of this work.

Abstract

The extensive micro fractures in wellbore formations tend to weaken the formation. Depending on wellbore pressures this can cause wellbore collapse or induce larger fractures that are susceptible to lost circulation. To maintain wellbore integrity and help prevent wellbore collapse, higher mud weights are typically recommended. However, increasing the mud weight may lead to other problems such as barite sag and excessive equivalent circulating density. The potential severity of these problems increases significantly in deviated wells or sensitive formations.

Gilsonite/Asphaltene-based products commonly referred to as “black powders,” have been applied successfully to improve wellbore stability. Gilsonite-based products extrude into micro fractures and plug them. This stops the transmission of wellbore pressure to formation. The ability to use these powders at higher temperatures adds to their versatility. The mechanism by which these products work is well understood, but the actual changes in formation properties and alteration in near-wellbore stress values has not been reported. Therefore, testing to determine the formation effects was performed using commonly available black powders. A standard static fluid loss test was performed, where fluid loss was monitored. Poro-elastic calculations were performed using a numerical simulator. Near-wellbore effective tangential stress was monitored for each case and significant improvement was observed for cases where black powder was used. The variation achieved in near-wellbore stresses when using black powder is presented along with the demonstration of how the product can be applied effectively for efficient drilling of a stable wellbore.

Introduction

Shales make up over 75% of the drilled formations, and over 70% of the borehole problems are related to shale instability resulting in downtime, excessive well construction costs, and lost production¹. Wellbore instability is a complex problem that includes rock mechanics, stress analysis, in-situ stress calculations, pore pressure prediction, and shale/fluid chemical reactions. Wellbore instability while drilling can take

many familiar forms such as stuck pipe, hole swelling, lost circulation, severely-enlarged hole or impaired directional control. Some related problems can arise when these wells are finally drilled to target, including uncertain formation evaluation, poor cementing, casing deformations, and ineffective perforating. Wellbore instability has become an increasing concern for horizontal and extended reach wells, especially with the move towards drilling completely open hole lateral sections, and in some cases, open hole build-up sections through shale formation.

Before a wellbore is drilled, rock is in a state of equilibrium. Downhole stresses on the rock under these conditions are known as the far field stresses (σ_v , σ_H , σ_h or *in-situ* stresses). The stress-strength imbalance comes about as rock is removed from the hole, replaced with drilling fluid, and the drilled formations are exposed to drilling fluids. Instances of wellbore instability will arise under the following conditions²:

“If the redistributed stress state exceeds the rock strength, either in tension or compression, then instability may result”.

Apart from in-situ stress values, formation properties such as mineralogy of shales, imbalance in activity of formation fluid and drilling fluid (activity is referred as amount of salt present in the fluid), permeability of the formation and presence of filter cake affects the required properties to drill a stable wellbore. Fluid pressure penetration near the wellbore which will result in a change in the effective stress³ that could potentially lead to the wellbore collapse and is controlled by two factors, permeability of formation and filter cake properties. Traditionally wellbore instability phenomena has been tackled by simply increasing the mud weight, however this approach does not always work. Micro fractures in shales are very commonly found and increasing mud weight for providing stability could instead lead to wellbore failure issues.

Wellbore stability analysis prediction involves determining the stress redistribution around the wellbore because of alteration in in-situ stress, by solving constitutive equations

with appropriate boundary conditions. Next step is to achieve the drilling fluid properties. Several authors published different techniques to maintain/achieve wellbore stability. *Ewy et.al.*⁴ studied the impact of wellbore pressure penetration into shale pore space and its impact on increase in near wellbore pore pressure and decrease in effective overbalance pressure for a water base mud. *Scorsone et.al.*⁵ illustrated the application of a gel system based upon polyurethane chemistry for wellbore stability and strengthening, where adhesion to impermeable formations is increased. *Zeilinger et.al.*⁶ utilized the concept of wellbore stability analysis observed in shale to design and implement a fluid system for drilling coal beds with micro fractures in the seams. Fluid loss was minimized by adding appropriate particle size lost circulation material (LCM), which in turn improved the wellbore stability. *Nguyen et.al.*⁷ performed numerical stress analysis for fractured shale formation. Dual porosity approach was used where fractures inside the shale formation was considered as a separate flow path and effect of several parameters on critical mud weight was determined. *Kang et.al.*⁸ developed a discrete element model (DEM) model to perform wellbore stability analysis. The model includes thermal, mechanical, chemical, and hydraulic effects between drilling fluid and formation and has the ability to perform post failure stress analysis. *Hemphill et.al.*⁹ performed experimental studies to determine the change in strength of shale samples and changes the water phase salinity of oil base mud to improve the wellbore stability. Porochemoelastic modeling was performed to analyze the effect of salinity on stress levels.

In this paper, application of black powders for enhancing wellbore stability while drilling with clay-free oil-based drilling fluid systems will be discussed. Formation of impermeable filter cake/plugging of the microfracture commonly found in shales and its implications on increase in near wellbore stress values will be presented. Wellbore stability analysis results will be presented which will give a overview of increased stability.

Wellbore Stability Analysis

*Terzaghi*¹⁰ proposed that an increase in pore pressure will decrease the effective stress. Effective insitu stress is determined by taking the pore pressure into consideration as described by equation

$$\sigma' = \sigma - p_p \quad \text{Eq 1}$$

To account for poroelastic behaviour of rock, *Biot's*¹¹ constant was introduced and the effective stress equation, Eqn 1 was modified as

$$\sigma' = \sigma - \alpha p_p \quad \text{Eq 2}$$

Principal stresses are stresses inclined at such angles, so that associated shear stress is zero. In the oil and gas industry, principal stresses are orthogonal to each other. For numerical calculation, these orthogonal stresses should be transformed to cylindrical coordinates. *Bradley*¹² proposed the transformation

matrix as written in Equation 3 (*See Appendix 1*) and has been widely used. Using Eqn 3, principal stresses are transformed to rectangular stresses.

Eqn 4 to Eqn 10 (*Refer Appendix 1*) can be used to transform stresses from rectangular coordinates to cylindrical coordinates (*Fjaer et. al.*¹³).

Special case of vertical wellbore ($i=0, \beta=0$)

Maximum value of effective tangential stress¹³ at the borehole wall is given by Eqn 11

$$\sigma_{\theta, \max} = 3\sigma_H - \sigma_h - p_w - p_p \quad \text{Eq 11}$$

and minimum value of effective tangential stress¹³ at the borehole wall is given by Eqn 12

$$\sigma_{\theta, \min} = 3\sigma_h - \sigma_H - p_w - p_p \quad \text{Eq 12}$$

where the maximum value occurs in the direction of σ_h and the minimum value in the direction of σ_H . Because of presence of natural fractures in the formation, generally the tensile strength of the formation is considered to be zero.

Boundary Conditions

At the interface of wellbore, two pressures act simultaneously: pore pressure and wellbore pressure. Depending on the permeability of the formation, boundary conditions are defined¹³. Permeable rock formation allows the mud to instantly flood the near wellbore region resulting in a constant pore pressure, which equals to the mud pressure. In impermeable rock formations, in spite of mud instantly flooding the near wellbore region, pore pressure does not become equal to wellbore pressure. Implications of these boundary conditions will be clear from following section:

Fracture initiation will always take place in the direction of minimum stress around the wellbore.

$$\sigma'_{\theta, \min} = 3\sigma_h - \sigma_H - p_w - p_p \quad \text{Eq 13}$$

The above equation does not account for temperature and salinity. Fracture will initiate only if the tangential stress around the wellbore becomes equal to or less than zero as given by Eqn 14.

$$\sigma'_{\theta, \min} \leq 0 \quad \text{Eq 14}$$

Applying the above condition, using Eqn 14 critical mud weight for fracturing permeable formations will be equal to Eqn 15,

$$p_w = \frac{3\sigma_h - \sigma_H}{2} \quad \text{Eq 15}$$

For impermeable formation critical fracturing mud weight will be equal to Eqn 16:

$$p_w = 3\sigma_h - \sigma_H - p_p \quad \text{Eq 16}$$

The most commonly drilled formation is shale and it is characterized by breaks along thin laminae or parallel layering or bedding less than one centimeter in thickness as shown in **Figure 1**. Because of the presence of breaks along the thin laminate, wellbore stability issues are very frequently encountered. During the drilling process, one can observe long angular cuttings at the shaker screen as shown in **Figure 2**, which primarily occur because of breaking of the formation. Using black powders will help ensure that these breaks along the laminate are plugged with the particles. Plugging also helps ensure that the rock becomes impermeable, thereby increasing the fracturing pressure and consequently the wellbore stability. Black powders also act as a filtration control additive. With less fluid loss to formation, no increase in pore pressure will be observed and using Eqn 1, there will be no decrease in effective stress around the near wellbore region.

To evaluate the effectiveness of black powder, a series of experiments and numerical calculations were performed as described in section below. Gilsonite/Asphaltene based black powder are commonly used. Different type of black powders along with their temperature limitations are shown in **Table 1**. They are very finely grinded powders having D10, D50 and D90 in the range of 2, 18 and 70 microns respectively.

Experimental Results and Discussions

Oil base mud (OBM) was formulated in lab by mixing desired additives in the appropriate quantity. For this study 11.5 ppg OBM with a 65/35 oil water ratio (OWR) was prepared. The fluid formulation is shown in **Table 2**. After the basic mud check was performed, the fluid was hot rolled for 16 hrs at 250 °F in a roller oven, after which a second mud check was performed (rheology, mud weight and electrical stability). To evaluate the effect of black powder on fluid loss, one specific grade of black powder was added to fluid at a different concentration. A constant pressure filtration technique was used for the experiment. High pressure / high temperature (HPHT) filtration tests were performed at 250 °F using filter paper and at a differential pressure of 500 psi for 30 minutes as recommended by API (*American Petroleum Institute*)¹⁴. Addition of black powder decreases the fluid loss, which is evident from **Figure 3**. Fluid loss under HPHT conditions decreases with increasing concentration of black powder. For the formulation containing 8.0 ppb of black powder, fluid loss measured in 30 minute was only 0.6 ml as compared to 4.0 ml for the base fluid (with no black powder).

To ensure the addition of black powder does not affect the rheology of fluid, different types of black powders were added to base fluid at a concentration of 6.0 ppb. Rheology was measured at different shear rates using a standard FANN® 35 SA rheometer. Plastic viscosity and yield point for different fluids were calculated using the Bingham plastic model and are plotted in **Figure 4** and **Figure 5**. No significant variation in plastic viscosity -was observed for different grades of black

powder used. Apart from fluid containing Black Powder 2, most of the other fluids had good yield point, indicating good hole cleaning properties. Low shear yield point for most of the fluids also had similar values as evident from **Figure 6**. Low shear yield point is associated with settling of higher specific gravity particles. Higher low shear yield point helps minimize particle settling. The 10 sec, 10 min and 30 min gel strength of the fluid containing black powder was also measured and has been plotted in **Figure 7**. Gel strength indicates how effectively the clays inside the fluid orient in such a way that they form networks. Because of these networks, cuttings can be suspended when the drilling fluid is in static condition. It is important to notice that the fluid used in this study did not contain any clay. Except for the fluid containing Black Powder 2, all other fluids exhibited similar gel strength over time.

Equivalent circulating density (ECD) was determined to understand the effect of the increased rheology. Calculated ECD is presented in **Figure 8**. A cuttings diameter of 0.25", pump rate of 500 gallons per minute (gpm), and drill pipe rotation at 120 rpm was assumed for the calculations. The density of fluid containing black powders is 11.5 ppg. From the calculations, it is evident that, for the assumed operating parameters, there is not a significant impact on ECD and the ECD stays below the fracture gradient of 12.5 ppg. From the above analysis, it can be inferred that addition of black powder has no detrimental effect on fluid rheology, and consequently, no significant increase in ECD was observed.

Wellbore Stability Analysis: Results and Discussions

Wellbore stability analysis primarily includes understanding the near wellbore stress value and estimating at what mud weight the formation can either go in shear failure or tensile failure mode. The process of drilling a well requires removal of rock from its position, and because of this stress redistribution takes place. Drilling fluid should be designed to minimize the difference in stresses around the wellbore and make the wellbore stable. Physiochemical interactions between drilling fluid and shale affect the stress values. A time-dependent analysis tool was used to perform wellbore stability analysis. The Drucker Prager shear failure model was used. Because of the presence of natural fractures or breaks in shales, the tensile strength of formation was considered to be zero. Other input parameters used for simulation are shown in **Table 3**. Calculations were performed for 1, 12, 24 and 240 hrs. To analyze the effect of black powder, two different types of formation were analyzed: **permeable** and **impermeable**. The implications of these conditions were discussed in the previous section.

For the permeable case, effective tangential stress near the wellbore region is negative, as shown in **Figure 9**. This implies that for the given mud weight/equivalent circulating density, tensile failure will occur. This could result from

pressure transmission which occurs because in the presence of fractures/breaks. With black powder in the drilling fluid, these fractures/breaks become completely sealed, making the formation impermeable. Effective tangential stress near the wellbore region is presented in **Figure 10**. It is evident that because of sealing of breaks/fractures, effective tangential stress near the wellbore becomes positive. Because of increased stress values, higher mud weight fluids can also be used to drill the section without experiencing stability issues.

The critical mud weight required for a stable wellbore under permeable and impermeable boundary conditions is presented in **Figure 11** and **Figure 12**. Four possibilities can be identified in the figure: stability, collapse, fracturing and collapse/fracturing. The area shaded in green in **Figure 11** and **Figure 12** is the stable area. As is evident from the figure, in the permeable case, the window for a stable wellbore is very narrow as compared to the impermeable case, where the stability window is very wide. The red shaded region indicates that the effective stress value goes beyond minimum horizontal stress, and in that case fracturing as well as collapse could be predicted.

The wellbore stability analysis tool could also be used to predict the best possible configuration (hole inclination and azimuth) so that an optimal mud weight could be selected to avoid any stability issues arising because of tensile fracturing or shear or collapse failure. **Figures 13 - 16** show 10 gradations across the radius and 36 gradations across the periphery. Each gradation represents 10 degrees. Gradation across the radius represents wellbore inclination and gradation across the periphery represents wellbore azimuth. **Figure 13** and **Figure 14** represent the critical mud weight required to prevent tensile fracturing and shear failure respectively for permeable case. The gray area on these charts indicates that irrespective of the mud weight, because of insitu stress, the wellbore will always be in failure mode. **Figure 15** and **Figure 16** represent the critical mud weight required to prevent tensile fracturing and shear failure respectively for impermeable case. Comparing **Figure 14** and **Figure 16**, in the impermeable case with no combination of wellbore inclination and azimuth, the well is in always fail mode. The impermeable critical mud weight below which shear failure will occur is significantly lower than the density in the permeable case. This increases the drilling window for the wellbore.

Conclusion

Experiments were performed to analyze the effect of gilsonite or asphaltene black powders on fluid loss and their ability to form filter cake. The following conclusions can be derived from the experimental results

1. Addition of black powder decreases the HPHT fluid loss value.
2. From the experimental data obtained, it is evident that additions of black powder do not affect the rheology of the fluid. The impact of different grades of black powders

on equivalent circulating density is also minimal.

3. Black powders do not increase the gel strength of the fluid. The fluid tested in this work contained no clays; additional study can be taken to analyze black powder effects on gel strength.
4. Because of the low fluid loss achieved with black powders, the resulting filter cake is tough and slick.
5. Wellbore stability analysis demonstrates enhanced stability of wellbore when black powders are used.
6. The upper and lower mud weight window increases, providing a wider drilling window when black powders are used.
7. The potential combinations of hole inclination and azimuth for drilling a stable wellbore increase when black powders are used.

Proper use of the wellbore stability analysis tool will help ensure selection of optimized mud weight for drilling a stable wellbore. Further studies could be undertaken to estimate the effect of the black powder on permeability reduction in the formation so that the formation damage potential could be known.

Acknowledgement

The authors would like to thank the management of Halliburton for permitting to present the work.

Nomenclature

ECD	---	Equivalent Circulating Density (ppg)
Δp	---	Pressure differential
ppg	---	Pounds per gallon (mud weight unit)
ppb	---	Pounds per barrel (concentration unit)
x, y, z	---	Axis in rectangular coordinates
r, θ, z	---	Axis in cylindrical coordinates
xy, yz, zx	---	Two dimensional planes
rr	---	Radial direction
zz	---	Axial direction
i	---	Wellbore inclination
β	---	Wellbore azimuth
θ	---	Angular position in a wellbore (deg)
σ	---	Stress (psi)
σ_v	---	Principal vertical stress (psi)
σ_H	---	Principal maximum horizontal stress (psi)
σ_h	---	Principal minimum horizontal stress (psi)
ν	---	Poisson's Ratio (---)
τ	---	Shear stress (psi)
$\theta \theta$	---	Direction tangent to wellbore radius
rr	---	Radial direction

References

1. Talabani S, Chukwu G, Hatziagniou, *Drilling Successfully Through Deforming Shale Formations: Case Histories*, SPE Rocky Mountain RegionaVLow Permeability Reservoirs Symposium, Denver, CO, U.S.A., April 12-14, 1993.
2. Pasic.B, G-Medimurec.N, Matanovic.D, *Wellbore instability: causes and consequences*, Rud.-geol.-naft. zb., Vol. 19, 2007.
3. McLellan, P.J., Wang, Y. *Predicting the effects of pore pressure*

penetration on the extent of wellbore instability: Application of a versatile poro-elastoplastic model, SPE-28053-MS, Rock Mechanics in Petroleum Engineering, 29-31 August 1994, Delft, Netherlands

4. Ewy, T.R, Morton.K. 2008. *Wellbore Stability Performance of Water Based Mud Additives*. Paper SPE 116139 presented at the SPE Annual Technical Conference and Exhibition held in Denver, Colorado, USA, 21-24 September.
5. Scorsone, T.J, Sanders, W.M, Patel, D.A. 2009. *An Improved Oil-Based Chemical Gel System for Wellbore Stabilization*. Paper SPE 121676 presented at the SPE International Symposium on Oilfield Chemistry held in The Woodlands, Texas, 20-22 April.
6. Zeilinger, S., Dupriest. F., Turton, R. Butler, H. Wang, H. 2010. *Utilizing an Engineered Particle Drilling Fluid to Overcome Coal Drilling Challenges*. Paper SPE-128715 presented at the IADC/SPE Drilling Conference and Exhibition held in New Orleans, Louisiana, USA, 2-4 February.
7. Nguyen, X.V, Abousleiman, N.Y, Hemphill, A.T. 2009. *Geomechanical Coupled Poromechanics Solutions While Drilling in Naturally Fractured Shale Formations With Field Case Applications*. Paper SPE-123901 presented at the SPE Annual Technical Conference and Exhibition held in New Orleans, Louisiana, 4-7 October.
8. Kang, Y., Yu, M., Miska, S., Takach, E.N. 2009. *Wellbore Stability: A Critical Review and Introduction to DEM*. Paper SPE-124669 presented at the SPE Annual Technical Conference and Exhibition held in New Orleans, Louisiana, 4-7 October.
9. Hemphill, T., Duran, W., Abousleiman, Y., Nguyen, V., Tran, M., Hoang, S. 2010. *Changing the Safe Drilling Window with Invert Emulsion Drilling Fluids: Advanced Wellbore Stability Modeling Using Experimental Results*. Paper SPE-132207 presented at the International Oil and Gas Conference and Exhibition in Beijing, China, 8-10 June.
10. Terzaghi, K. 1943. *Theoretical Soil Mechanics*. New York: John Wiley.
11. Biot, M. A. 1955. *Theory of elasticity and consolidation for a porous anisotropic soil*. Journal of Applied Physics 26(2):182–185.
12. Bradley, W. B. 1979, *Failure of Inclined Boreholes*. Transactions of the ASME, Vol. 101 (Dec. 1979) 232.
13. Fjaer, E., Holt, M. R., Horsrud, P., Raen, M. A., Risnes, R. 2008. *Petroleum Related Rock Mechanics*. 2nd Edition. Amsterdam: Elsevier.
14. *Recommended Practice for Laboratory Testing of Drilling Fluids*, API Recommended Practice.

Table1: Application and temperature limit of black powder used in this study

	Application	Temp (°F) Limit
Black Powder 1	Filtration Control/Shale Stabilizer	400
Black Powder 2	Filtration Control/Shale Stabilizer	350
Black Powder 3	Filtration Control/Shale Stabilizer	400
Black Powder 4	Filtration Control/Shale Stabilizer/Cutting dispersion inhibitor	400
Black Powder 5	Filtration Control/Shale Stabilizer	500
Black Powder 6	Filtration Control/Shale Stabilizer	500

Table 2: Formulation of invert emulsion fluid

Specification	
Mud weight	11.5 ppg
Oil water ratio	65/35
Water phase salinity	250000 ppm
Components	Concentration, ppb
Base Oil	As required
Emulsifier	9
Lime, ppb	1.5
Filtration Control	2
Viscosifier 1	2
Viscosifier 2	6
Black Powder	6
Water, bbl	0.297
Calcium chloride, ppb	30.4
Ground Marble	25
Barite	As required

Table 3: Data used for wellbore stability analysis.

Borehole Data	
Hole Inclination (deg)	0
Hole Azimuth (deg)	0
Borehole radius (inches)	4.25
TVD (feet)	8000
Mud Weight/ECD (ppg)	12
In Situ Stress Gradients	
Vertical Stress (psi/ft)	0.88
Max Horizontal Stress (psi/ft)	0.83
Min Horizontal Stress (psi/ft)	0.65
Pore Pressure (psi/ft)	0.442
Maximum Horizontal Stress (deg)	0

Rock Properties	
Cohesion (psi)	1267
Friction Angle (deg)	30
Tensile Strength (psi)	0
Young's Modulus (psi)	1.00E+06
Poisson's Ratio (---)	0.22
Formation Permeability (mD)	1.00E-04
Time	
Time1 (hrs)	1
Time2 (hrs)	12
Time3 (hrs)	24
Time4 (hrs)	240

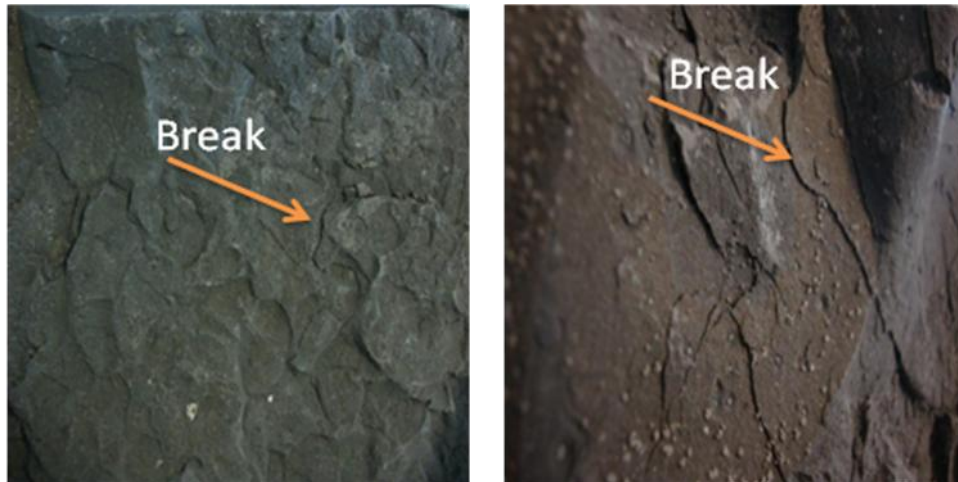


Figure 1. Breaks/fractures observed in the thin laminate of shales



Figure 2: Long angular cuttings are observed at the shaker screen because of wellbore instability

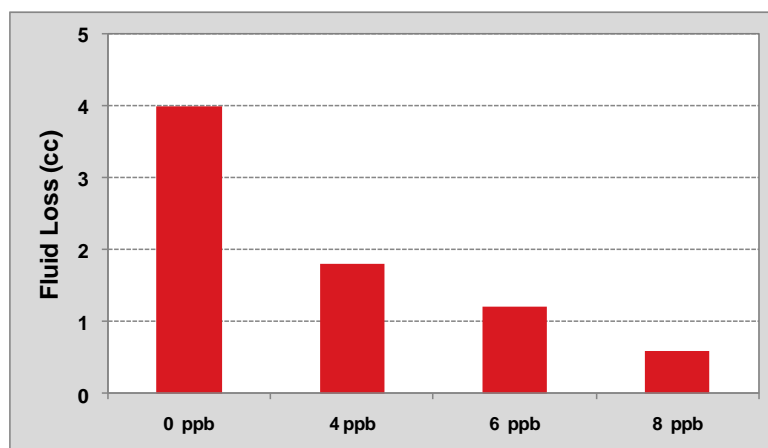


Figure 3: HTHP fluid loss (250 F /500 psi) using Black Powder 2.

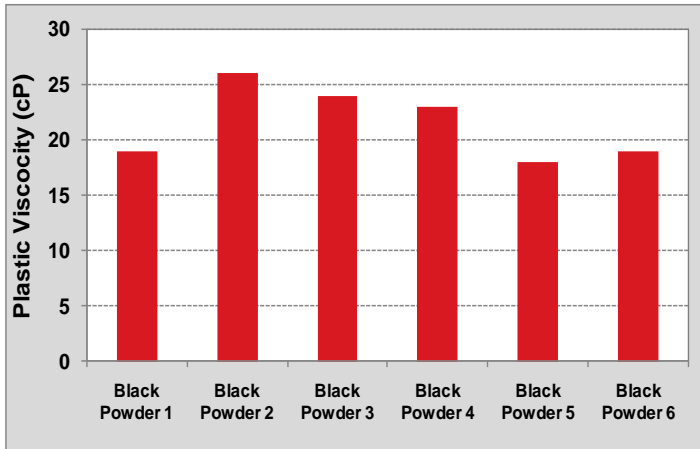


Figure 4: Plastic viscosity of drilling fluid after adding 6 lb/bbl of different black powder

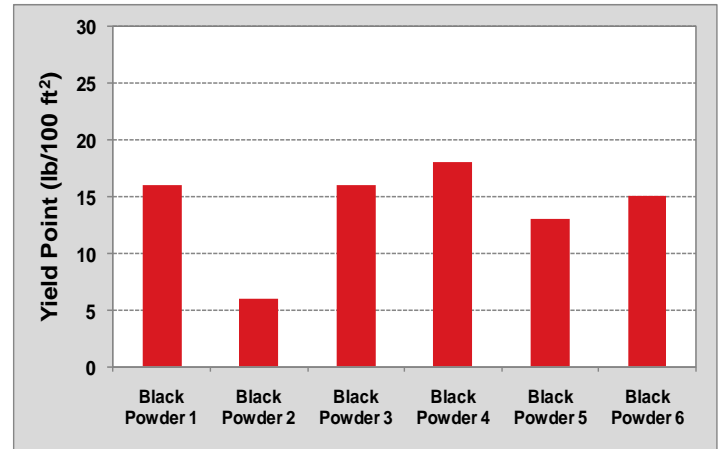


Figure 5: Yield Point of drilling fluid after adding 6 lb/bbl of different black powder

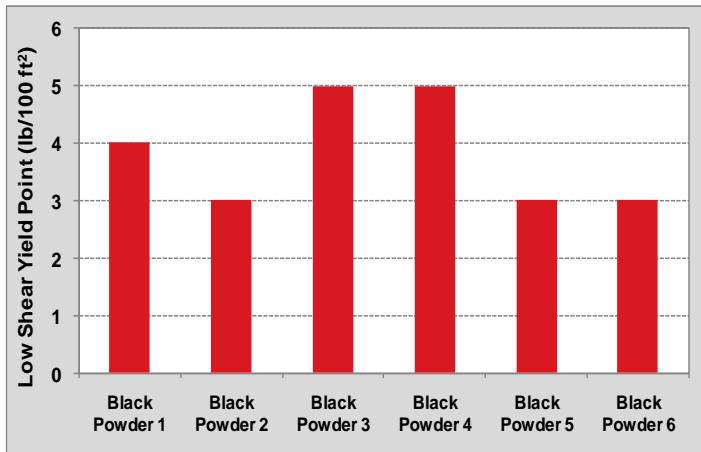


Figure 6: Low Shear Yield Point of drilling fluid after adding 6 lb/bbl of different black powder

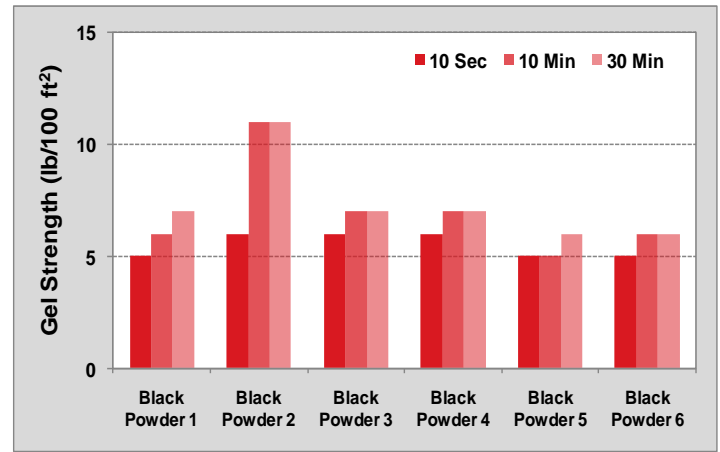


Figure 7: Gel Strength of drilling fluid after adding 6 lb/bbl of different black powder

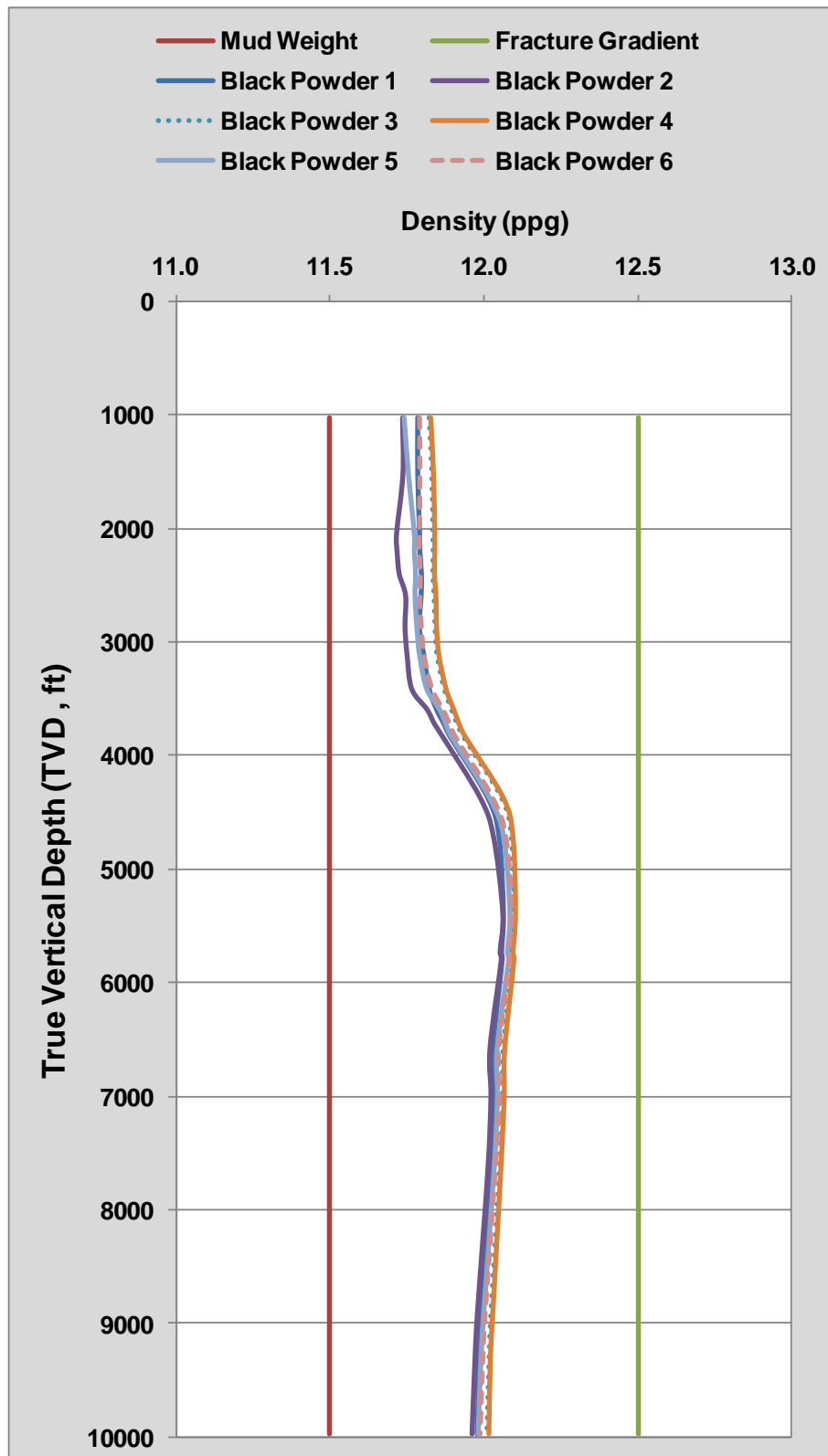


Figure 8: Predicted equivalent circulating density for fluids containing 6ppb of black powder.

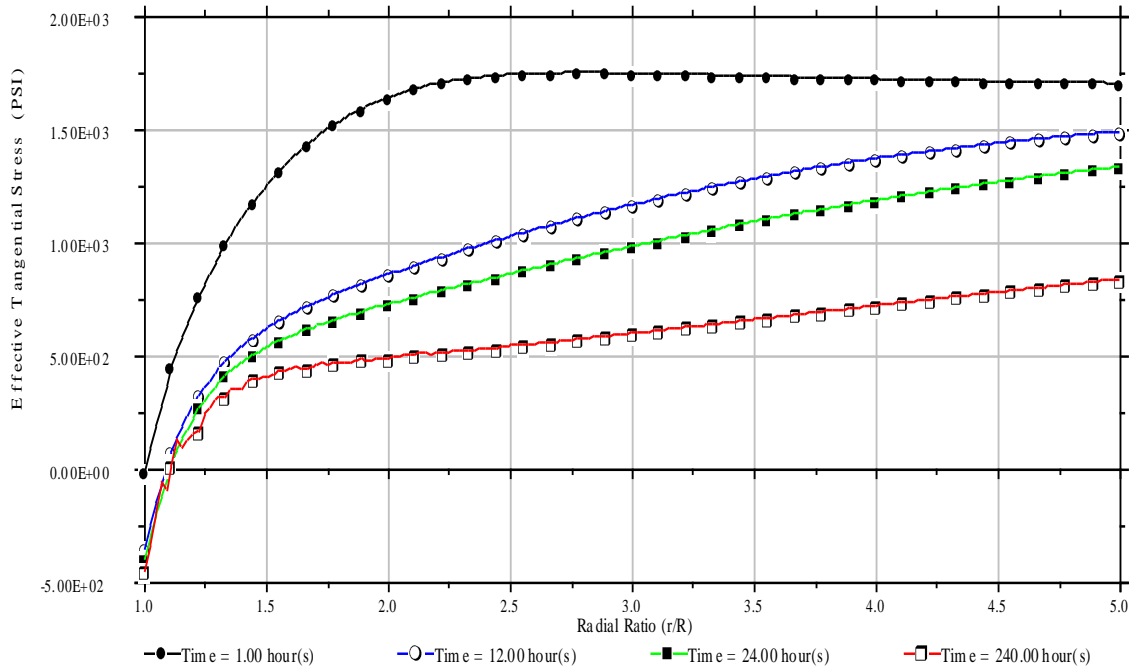


Figure 9: Effective tangential stress for permeable boundary condition. Stress value becomes negative in the near wellbore region indicating probability of tensile failure.

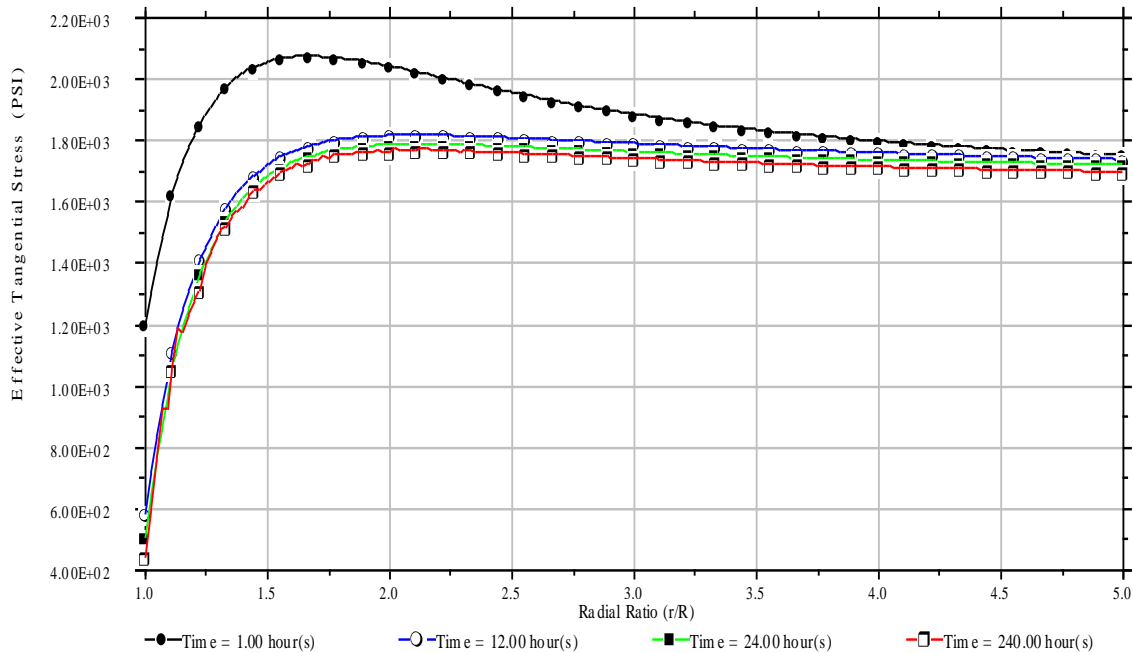


Figure 10: Effective tangential stress for impermeable boundary condition. Stress value stays positive in the near wellbore region indicating a stable wellbore.

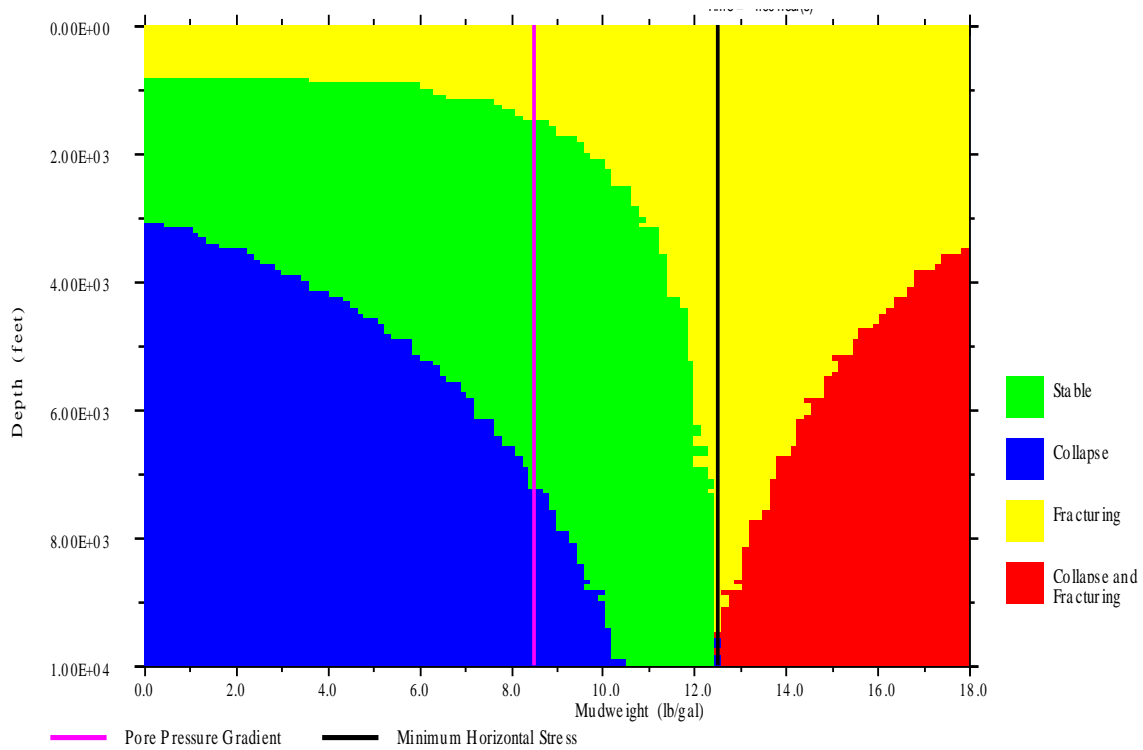


Figure 11: Critical mud weight required for a stable wellbore for permeable boundary condition with varying depth. Green color indicates stable wellbore. Area shaded in red regions indicates unstable wellbore.

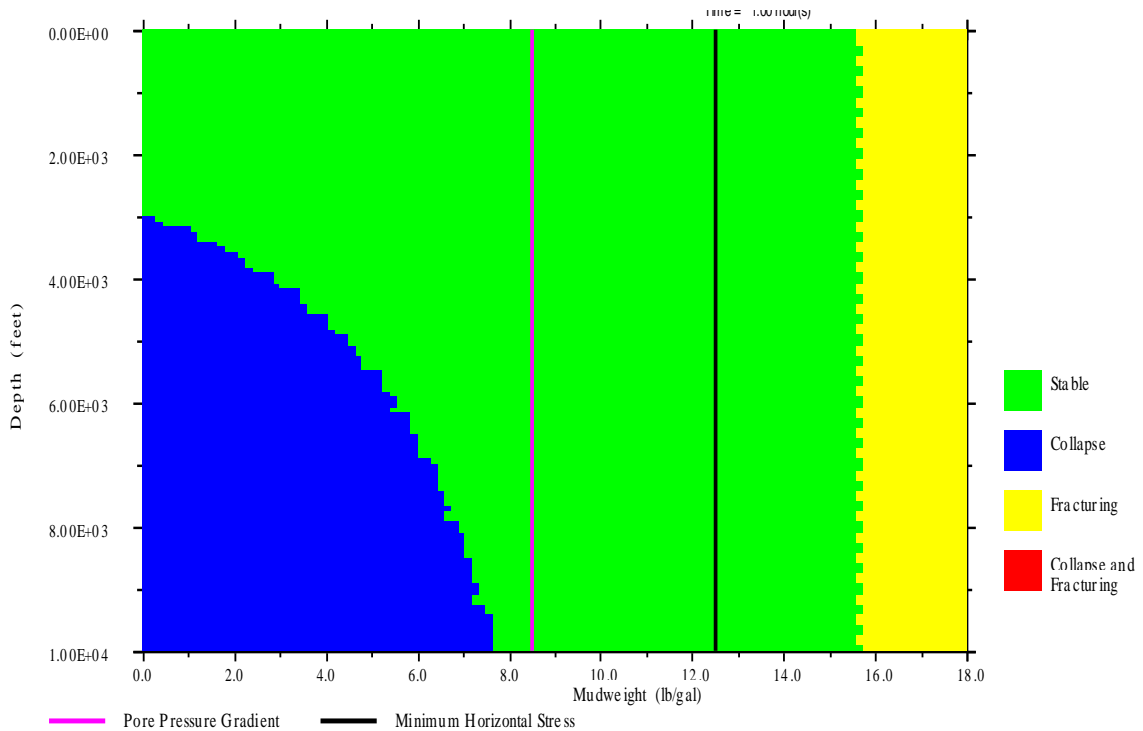


Figure 12: Critical mud weight required for a stable wellbore for impermeable boundary condition with varying depth. Green color indicates stable wellbore.

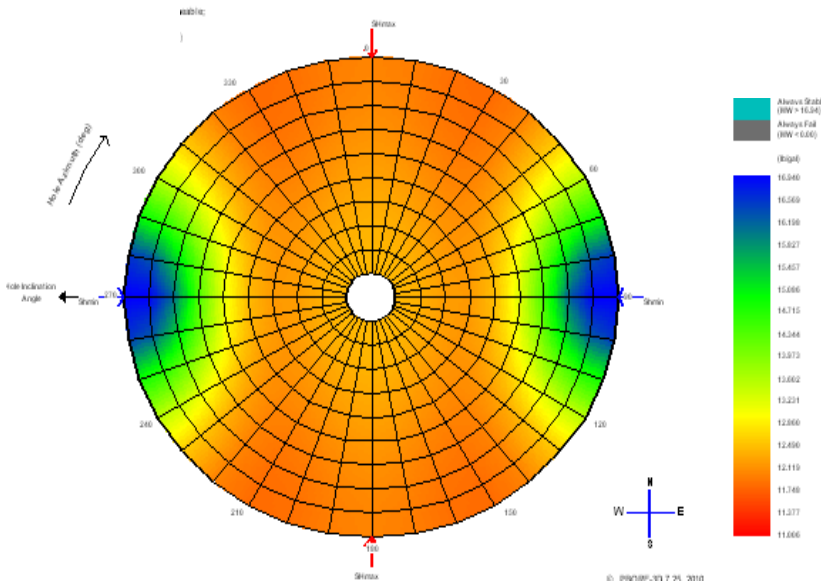


Figure 13: Critical mud weight required to prevent tensile fracturing for permeable case.

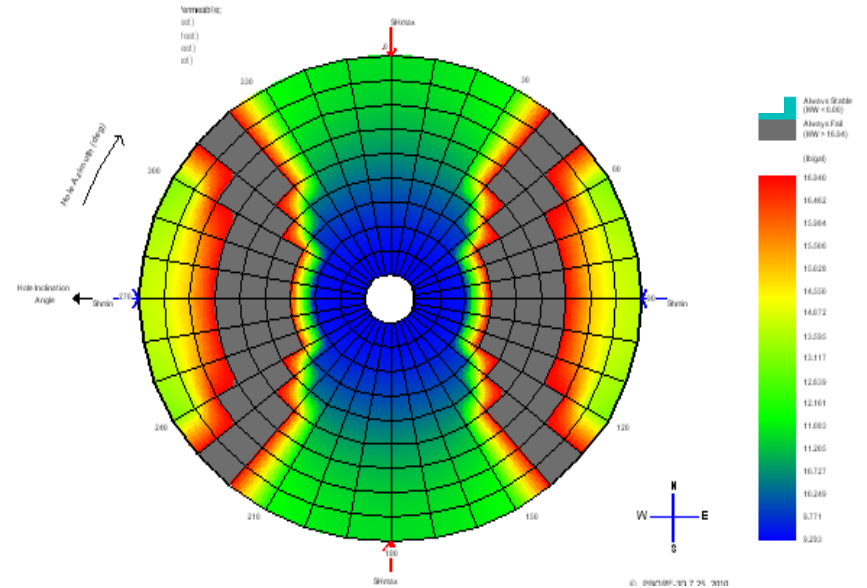


Figure 14: Critical mud weight required to prevent shear failure for permeable case.

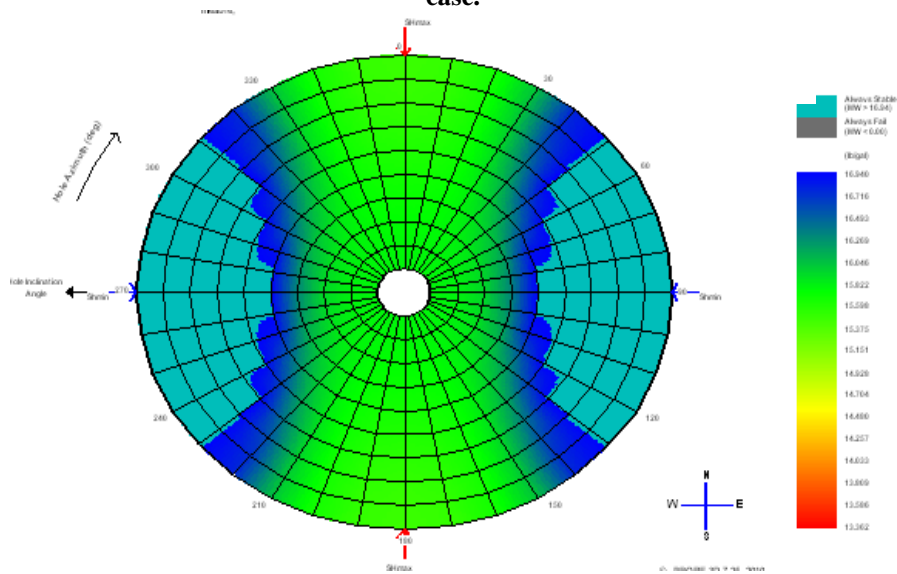


Figure 15: Critical mud weight required to prevent tensile fracturing for impermeable case.

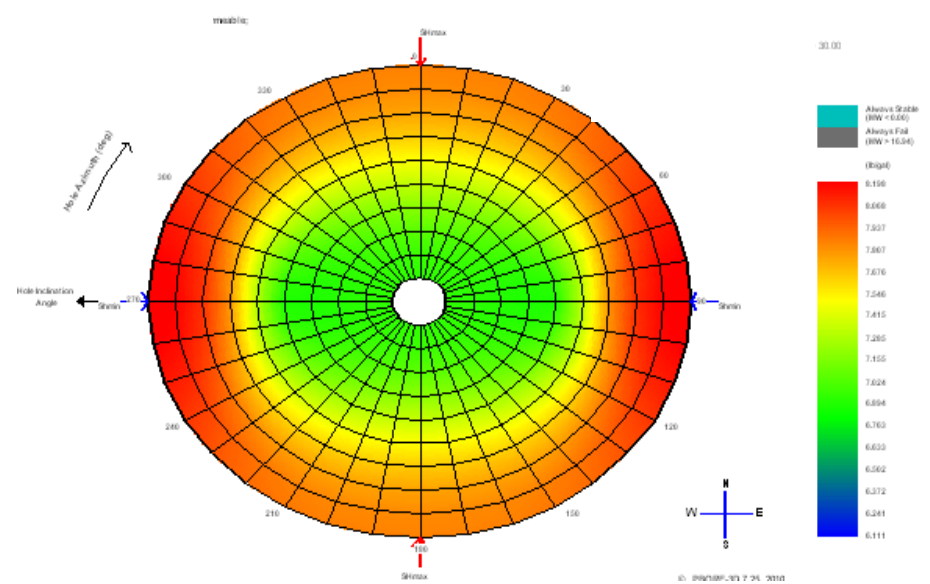


Figure 16: Critical mud weight required to prevent shear failure for impermeable case.

Appendix 1:

$$\begin{bmatrix} \sigma_x \\ \sigma_y \\ \sigma_y \\ \tau_{yz} \\ \tau_{xz} \\ \tau_{xy} \end{bmatrix} = \begin{bmatrix} \sin^2 \beta & \cos^2 \beta \cos^2 i & \cos^2 \beta \sin^2 i \\ 0 & \sin^2 i & \cos^2 i \\ \cos^2 \beta & \sin^2 \beta \cos^2 i & \sin^2 \beta \sin^2 i \\ 0 & -\sin i \cos i \sin \beta & \sin i \cos i \sin \beta \\ -\sin \beta \cos \beta & \sin \beta \cos \beta \cos^2 i & \sin \beta \cos \beta \sin^2 i \\ 0 & -\sin i \cos i \cos \beta & \sin i \cos i \cos \beta \end{bmatrix} \begin{bmatrix} \sigma_V \\ \sigma_H \\ \sigma_h \end{bmatrix} \quad \text{Eqn 3}$$

$$\sigma_r = \frac{\sigma_x + \sigma_y}{2} \left(1 - \frac{r_w^2}{r^2}\right) + \frac{\sigma_x - \sigma_y}{2} \left(1 + 3\frac{r_w^4}{r^4} - 4\frac{r_w^2}{r^2}\right) \cos 2\theta + \tau_{xy} \left(1 + 3\frac{r_w^4}{r^4} - 4\frac{r_w^2}{r^2}\right) \sin 2\theta + (p_w - \alpha p_p) \frac{r_w^2}{r^2} \quad \text{Eqn 4}$$

$$\sigma_r = \frac{\sigma_x + \sigma_y}{2} \left(1 - \frac{r_w^2}{r^2}\right) + \frac{\sigma_x - \sigma_y}{2} \left(1 + 3\frac{r_w^4}{r^4} - 4\frac{r_w^2}{r^2}\right) \cos 2\theta + \tau_{xy} \left(1 + 3\frac{r_w^4}{r^4} - 4\frac{r_w^2}{r^2}\right) \sin 2\theta + (p_w - \alpha p_p) \frac{r_w^2}{r^2} \quad \text{Eqn 5}$$

$$\sigma_\theta = \frac{\sigma_x + \sigma_y}{2} \left(1 + \frac{r_w^2}{r^2}\right) - \frac{\sigma_x - \sigma_y}{2} \left(1 + 3\frac{r_w^4}{r^4}\right) \cos 2\theta - \tau_{xy} \left(1 + 3\frac{r_w^4}{r^4}\right) \sin 2\theta - (p_w - \alpha p_p) \frac{r_w^2}{r^2} \quad \text{Eqn 6}$$

$$\sigma_z = \sigma_z - \nu \left(2(\sigma_x - \sigma_y) \frac{r_w^2}{r^2} \cos 2\theta + 4\tau_{xy} \frac{r_w^2}{r^2} \sin 2\theta\right) \quad \text{Eqn 7}$$

$$\tau_{r\theta} = \left(\frac{\sigma_y - \sigma_x}{2}\right) \left(1 - 3\frac{r_w^4}{r^4} + 2\frac{r_w^2}{r^2}\right) \sin 2\theta + \tau_{xy} \left(1 - 3\frac{r_w^4}{r^4} + 2\frac{r_w^2}{r^2}\right) \cos 2\theta \quad \text{Eqn 8}$$

$$\tau_{\theta z} = \left(-\tau_{xz} \sin \theta + \tau_{yz} \cos \theta\right) \left(1 + \frac{r_w^2}{r^2}\right) \quad \text{Eqn 9}$$

$$\tau_{rz} = \left(\tau_{xz} \cos \theta + \tau_{yz} \sin \theta\right) \left(1 - \frac{r_w^2}{r^2}\right) \quad \text{Eqn 10}$$